Carbon Nanotube-based Black Coatings for Optical and Infrared Applications

By D. Carnahan and T. Morgan
NanoLab, Inc.

The search for the blackest of black pigments is likely now at its end, or nearly so, with the development of carbon nanotube-based paints that swallow more than 99% of light across the visible spectrum.

From the very first paints to today, the discovery and development of the purest of materials and pigments has been a goal for artists and designers alike. The search for the blackest of black pigments is likely now at its end, or nearly so, with the development of carbon nanotube-based paints that swallow more than 99% of light across the visible spectrum.

The focus of our paint development over the last five years has been on creating the blackest matte-black paints using carbon nanotubes and tailoring them for use across the ultraviolet, visible, and infrared. Vertically aligned carbon nanotube arrays (VANTA) hold the record as the world's blackest, most highly absorbing materials, and this is due both to their chemical composition and their structure. The optical properties of carbon nanotubes are crystallographically dependent, as their structure is highly anisotropic. Nanotubes are similar to graphite, which has different in-plane and thru-thickness optical constants, except that in carbon nanotubes, the planes are wrapped into a tubular shape. As a result, VANTA coatings are not very black at grazing-angle incidence, due to that structural anisotropy. The VANTA coatings are synthesized at >500 °C, limiting the materials that can host such a material.

To address this and other issues, we have researched and developed optically absorbing carbon nanotube-loaded paints (now marketed as Singularity Black). These use a more randomized structure that has been tailored for high-optical and infrared absorption at normal and grazing-angle incidence. This paper describes the structures necessary for highly absorbing black coatings and reviews the approach and data collected for two products, Singularity Black paint, and our version of vertically aligned nanotube arrays, adVANTA.

Optical

INTRODUCTION

The creation of a fully matte, black paintable coating with absorption exceeding 99% in the visible requires not just selection of fillers and binders, but also the structure of the surface that will minimize reflection. Our approach in developing an exceptionally matte, black paint required that we optimize each step of light's interaction with a material.

As light interacts with a material, all of its energy is either reflected back from, or refracted into, the material, where it can then be transmitted or absorbed. The optical engineer's first goal in creating a black coating is to drive surface reflection to zero. As light crosses the boundary from one medium to another, the magnitude of the refractive index mismatch drives the amount of light reflected. The reflectivity R, the amount of light that is reflected at an interface, is related to the refractive indices n_1 and n_2 of the materials, and the incidence angle with the Fresnel equations, which for normal incidence reduces to

$$R = \frac{(n_1 - n_2)^2}{(n_1 + n_2)^2} \qquad (1)$$

If we consider light in air or vacuum (n_1=1) encountering glass (n_2=1.5), the reflected energy will be ~4% of the incident energy at one interface. If we consider other angles of incidence, the light polarization comes into play, and the reflectance becomes

$$R_\perp = \left(\frac{(\cos\theta - \sqrt{n_{21}^2 - \sin^2\theta}}{\cos\theta + \sqrt{n_{21}^2 - \sin^2\theta}} \right)^2 \quad \& \quad R_\parallel = \left(\frac{n_{21}^2 \cos\theta - \sqrt{n_{21}^2 - \sin^2\theta}}{n_{21}^2 \cos\theta - \sqrt{n_{21}^2 - \sin^2\theta}} \right)^2 \qquad (2)$$

Here n_{21} is the ratio of n_2 to n_1, and the sum of the two components equals the total reflectivity. For the time being, we will restrict the discussion to normal incidence. Maxwell's equations tell us that the refractive index n is the square root of the dielectric constant ε_r. With a more thorough examination, we recognize that the refractive index has both real and imaginary components (n and k, respectively), which are similarly related to the complex dielectric function with its real ε' and imaginary parts ε'', which can have frequency (w) dependence

$$(n + ik)^2 = \varepsilon' + i \cdot \varepsilon'' \qquad (3)$$

The imaginary or loss component of the dielectric function is related to conductivity (σ) by

$$\sigma(\omega) = \omega \cdot \varepsilon''(\omega) \qquad (4)$$

Combining and rearranging these terms, we have

$$(n + ik)^2 = n^2 + k^2 + i \cdot 2nk = \varepsilon' + i \cdot \frac{\sigma}{\varepsilon_0 \cdot \omega} \qquad (5)$$

From eq 5, we can expect that highly conductive materials, like metals, will have a huge refractive index, and therefore high reflectivity from eq 1. Specular reflection occurs in smooth metal surface so beautifully because the light waves do not penetrate beyond a skin depth, and are re-emitted without significant absorption. Metals, having no band gap, will interact with any incident photon to excite an electron from the valence band to the conduction band, which can then undergo direct relaxation, re-emitting a photon of nearly the same energy. Conversely, insulators may have high real dielectric constants, owing to their polarizability, so in turn they can have high refractive index values. However, for materials having only moderate conductivity and low polarizability, we can minimize refractive index, and thereby reduce reflection.

Materials and Dielectric Constant

The dielectric constant of a material is determined by the sum of several contributing polarization types, which in turn are related to the structure and bonding between atoms. Strong covalent bonds, such as that between carbon atoms, have low electronic polarizability, compared with the more ionic bonds present in oxides and halides.

However, the only strategy to reduce the reflectivity that we can employ for most materials (which have index values larger than 1), is to add porosity and/or surface roughness. Further, that porosity or roughness should be small relative to the wavelength of light. Such a nanoporous structure can now effectively have an index that approaches that of air. In practice, we find our best-performing surfaces have a distribution of pore sizes below 20 μm. Only a few super-porous materials can be readily synthesized. These include aerogels, zeolites, whisker, and nanofiber structures. Nature utilizes this approach, as is evidenced in the light-gathering structures of moth eyes, and various spiders and bird plumage.[1] Moth eye structures can be manufactured with arrays of protuberances having dimensions smaller than the wavelength of the light incident upon them and a thickness greater than the wavelength to maximize absorption. These structures form a region of graded refractive index at the interface between two media, and they are highly effective at reducing the amount of reflected light. If a highly matte, absorbing painted coating is desired, it is essential to find a way for the dried/cured surface to mimic these nanoporous, rough structures. While these structures encourage light to enter a coating, it is the material properties of the absorbers, or pigments and binders, that drive the effectiveness of absorption.

For materials with large band gaps, the optical light energy is insufficient to promote electrons to the conduction band, so light travels through without absorption. We call this state "transparency." Materials with midsize band gaps can create colors, as some wavelengths are absorbed, while others pass through. But it is the lossy materials, those with small band gaps, which are useful for the physicist or engineer who wants to create good black materials. Materials with a very small or nonexistent band gap are favored, as they can interact with all the incident energy, but those materials that undergo nonradiative recombination, i.e., those that relax through phonon interactions instead of re-radiation of photons are best. Fe_3O_4 is one such material, with a band gap of 0.1 eV, and heavily doped silicon is another. Both have been used for black coatings. Taken together, a near-ideal absorber would be created from a low-band-gap material that is capable of being formed into a highly nanoporous structure.

Carbon nanotubes (CNTs) have been a fascination for materials scientists since their discovery in 1991. The characterization of their properties, understanding of how to best produce these materials, and the development of strategies for their chemical modification and incorporation into composites has taken nearly 30 years to mature. Originally found as random soots in arc reactors, they were impure and difficult to isolate. Chemical vapor deposition (CVD) processes then solved the problems of bulk production, and alongside that development was the discovery of VANTA growth from catalyzed substrates. While nanotube arrays made by plasma-enhanced CVD are quite vertical, those made by thermal CVD have imperfect alignment, as they lack an organizing force, but are aligned roughly during growth by neighbor-to-neighbor interactions. As grown, VANTA arrays are 3–5 vol % dense, so nanotube-to-nanotube spacing can be 15–50 nm. A scanning electron microscope (SEM) image from a 16 μm tall adVANTA array is given in *Figure 1*.

The light-absorbing properties of nanotubes, particularly those of aligned nanotubes, were noted in the late 1990s.[2] However, processing and other hurdles delayed the exploration of this material as a black coating for the optics community for several years. In 2011, NanoLab was awarded a NASA Small Business Innovation Research (SBIR) contract to explore avenues to create tougher, more flexible, and adherent VANTAs for use in starlight suppression. As we developed aligned arrays with better and better optical properties, we observed that the grazing-angle performance of these arrays was relatively poor.

Bao, Ran, and Fisher modeled the directional components that make up nanotube dielectric response of an aligned array of CNTs, which is depicted in *Figure 2*.[3] When light interacts with a nanotube end-on, the real and imaginary components of the dielectric constant are both near 2 and are flat across the optical spectrum. However, when light interacts with a nanotube perpendicular to its axis, it is easier to stimulate carriers in that direction, and the real and imaginary components are larger. From this analysis, we can see why an aligned array of CNTs has excellent optical absorbance for near perpendicular angles of incidence, but for grazing angles, we see markedly higher index, and therefore larger mismatch and more reflection.

Armed with this estimate of the refractive index given by randomly entangled CNT, (n~1.9, k~2.1) we then added significant porosity to the model to approximate the structure that is generated in unaligned coatings. The following review is a comparison of aligned nanotube arrays and the unaligned structures that were created.

METHODOLOGY

Two materials were prepared for the comparative experiments conducted herein.

Titanium foil, mica, and stainless-steel foils (McMaster Carr) were purchased and cleaned using an RCA-1 protocol (80 °C- 5-min immersion in an 80C solution of 5 H_2O, 1 H_2O_2, 1 NH_4OH), then rinsed with DI water, and dried under flowing nitrogen. The substrates were then mounted on a platen and inserted into a Lesker PVD 75 sputtering system. After pump down, the pressure in the chamber was adjusted to 5 mT with flowing argon and oxygen in a molar ratio of ~15:1. A DC sputter gun equipped with an aluminum target was energized to 185W for ~7 min, sufficient to deposit a 10 nm layer of reactively sputtered aluminum oxide, as measured by a quartz crystal thickness monitor in the system. Next, the system was pumped back down, and the 5 mT pressure reestablished with argon only. A second sputtering gun was energized to 100W for ~1 min, sufficient to deposit 1 nm iron atop the alumina. Substrates were then removed from the system and cleaved for growth experiments.

One of the Thermal Chemical Vapor Deposition systems consisted of a 3-in.-diameter quartz-tube furnace, plumbed for Ar, H_2, and C_2H_4. Cut substrates were first calcined in air at 500 °C for 2 min to oxidize the iron catalyst layer and stabilize it for heat-up. Once calcined, the substrates were sealed in the tube

FIGURE 1—SEM image of a cleaved adVANTA array showing the overall alignment and density of CNT.

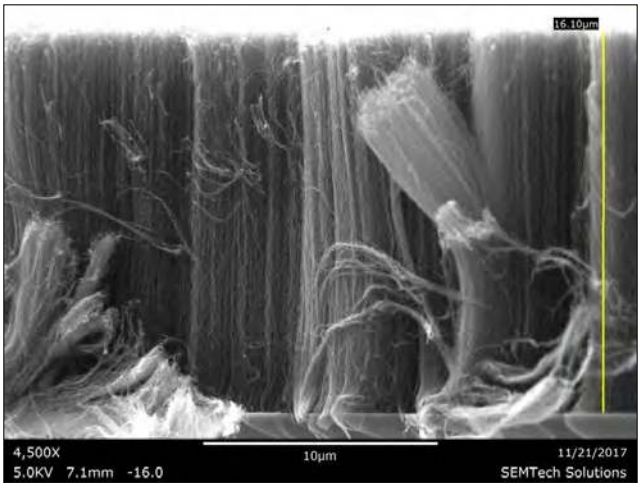

furnace vestibule while the furnace was heated to 730 °C. At temperature, the substrates were introduced to the hot zone and reduced for 1.5 min in flowing argon and hydrogen, typically at a 5:1 ratio. After reduction, ethylene was added to the flowing argon and hydrogen to initiate nanotube growth. These conditions were held for ~30 min, sufficient to create a carpet of nanotubes ~400 μm tall. These were cooled in argon, and then stored for analysis.

Separately, bulk CNTs, produced by chemical vapor deposition at NanoLab (product code PD15L5-20) were purified using full-strength hydrofluoric and hydrochloric acids (Alfa Aesar), then rinsed with DI water until a neutral pH was obtained. Nanotubes were then dried and reground to a powder. Thermogravimetric analysis confirmed the purity at >95 wt %. The nanotubes were then ultrasonically dispersed in tetrahydrofuran (THF, Sigma Aldrich) using a nonionic surfactant and added to a solution containing a proprietary polymer and a crosslinking agent. The resulting black suspension was stable and readily sprayed with an Iwata Eclipse hobbyist airbrush. Stainless steel, or SS, (304) and 6061 aluminum sheets were cut to 1-in. squares, then airbrush spray-coated, using approximately 10 ml of the suspension each, sufficient to leave an opaque, tough film on the substrates. Samples were left to dry overnight, then heated to 120 °C using a heat gun. This was sufficient to crosslink the polymer, fixing the highly porous network as shown in *Figure 3*. Residuals left behind after the polymeric decomposition and the crosslinker serve to bond the remaining CNT structure together in this formulation. A series of SEM images of the network

FIGURE 2—At left, Fisher's group used FTDT simulations to model the dielectric function of CNTs.[3] Using that data, at right, we calculated the complex refractive index at 550 nm and estimate the index for a 45° condition analogous to a randomly aligned structure.

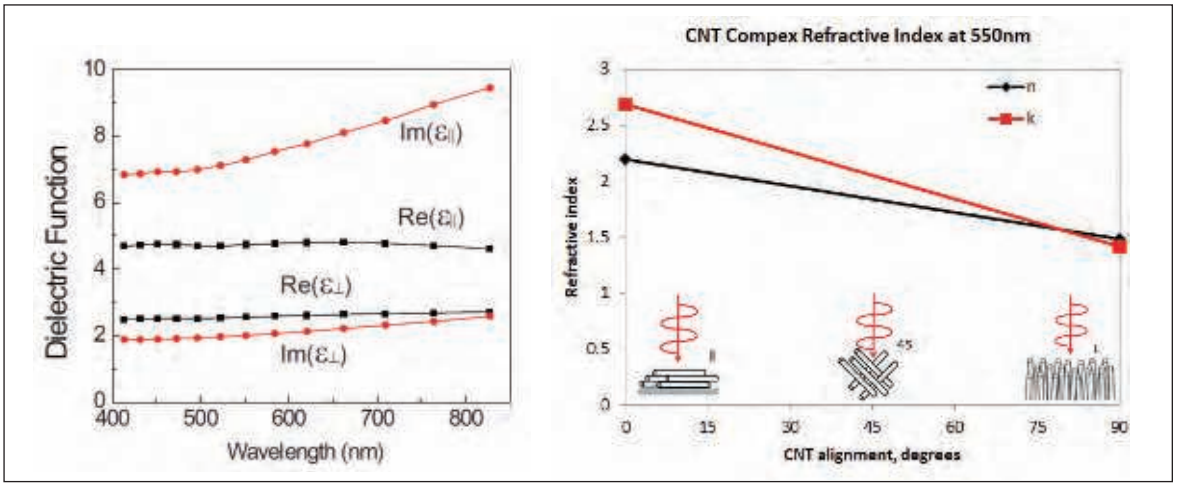

FIGURE 3—When heated, the crosslinker and polymer bond strongly, locking the CNT in a porous network.

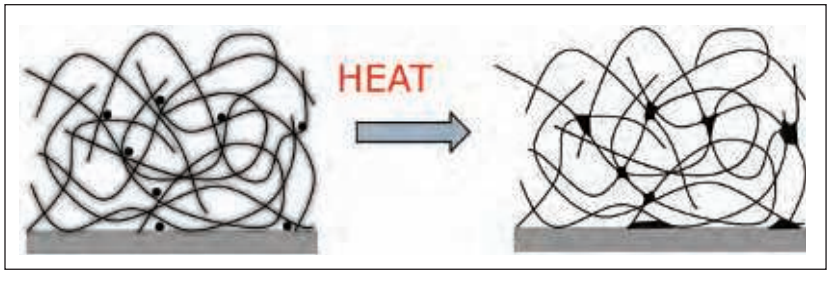

FIGURE 4—Sequence of magnifications, showing the CNT network porosity at multiple size scales.

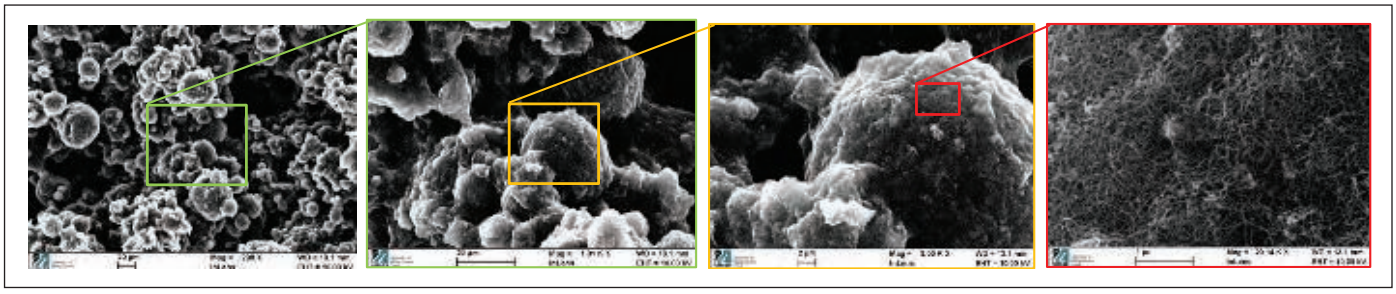

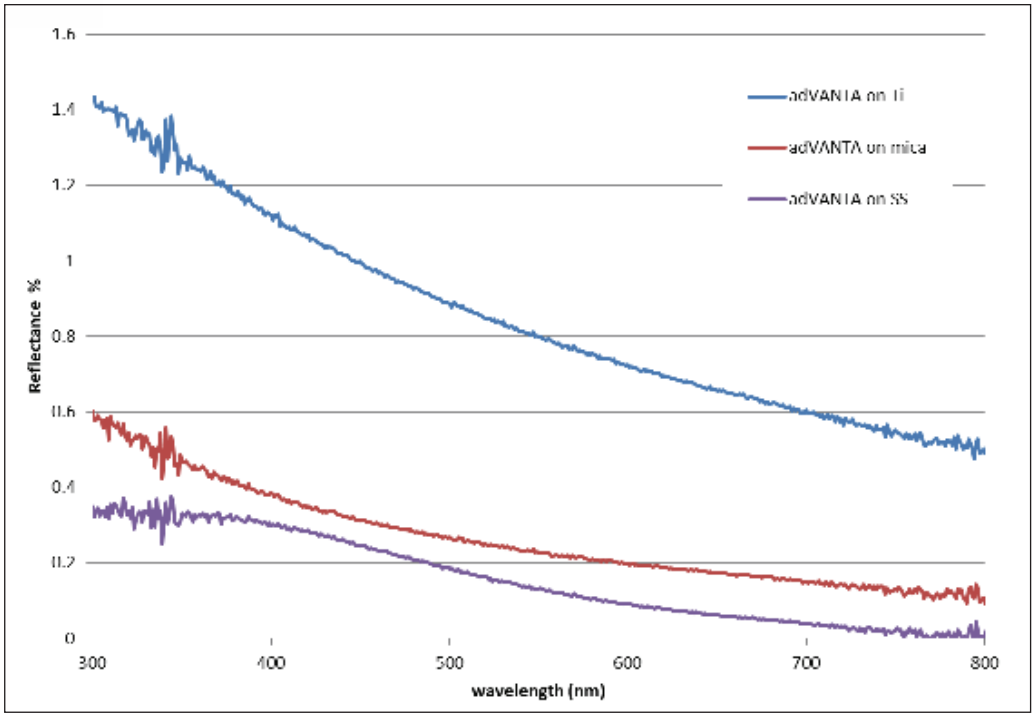

FIGURE 5—THR of several adVANTA coatings grown on several substrates.

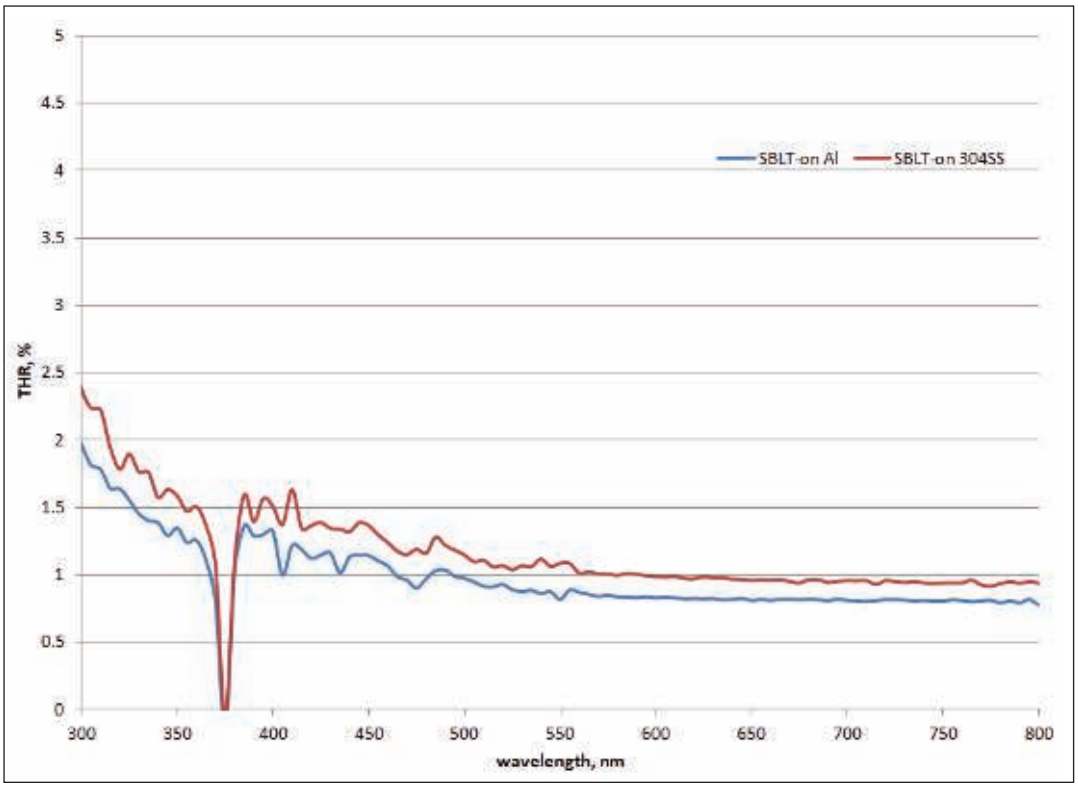

FIGURE 6—THR for Singularity Black coatings on stainless steel and aluminum.

is shown in *Figure 4*. Pore sizes in this structure range from 40 µm to 50 nm. The volume fraction of CNT in the network is approximately 20%.

DATA

The optical and infrared (IR) properties of both VANTAs and the prepared optical paint were analyzed at normal and grazing-angle incidence. A Perkin Elmer Lambda 19 UV-Vis spectrometer, equipped with a 60 mm integrating sphere was used to collect Total Hemispherical Reflectance (THR) data for aligned arrays grown on Ti, SS, and mica sheets. The data for the thermal CVD VANTA arrays is given in *Figure 5*. The same system was then used to characterize the sprayed coatings on aluminum and SS sheets, and that data is given in *Figure 6*. A lamp change at ~380 nm causes some instability in the measurement at that wavelength.

To analyze the IR properties of these materials, a diffuse reflectance accessory (Pike EZ-Diff) was purchased and installed in a Perkin Elmer FTIR 2000. The diffuse reflectance was then collected for the various films, between 2 and 12

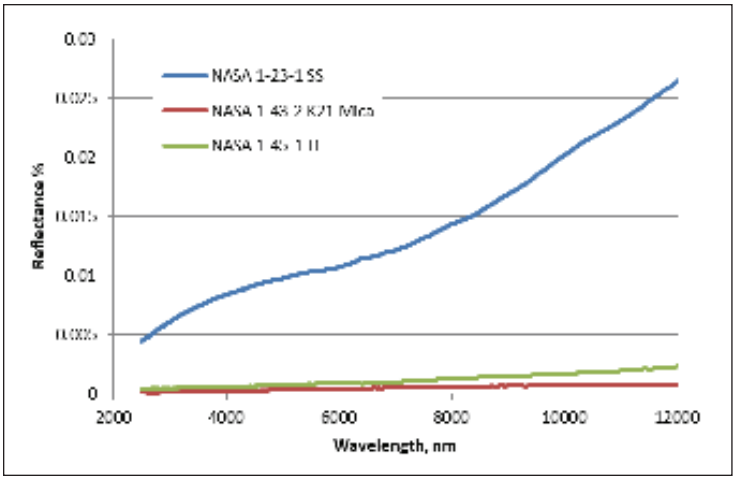

FIGURE 7—DRIFTS data for adVANTA arrays.

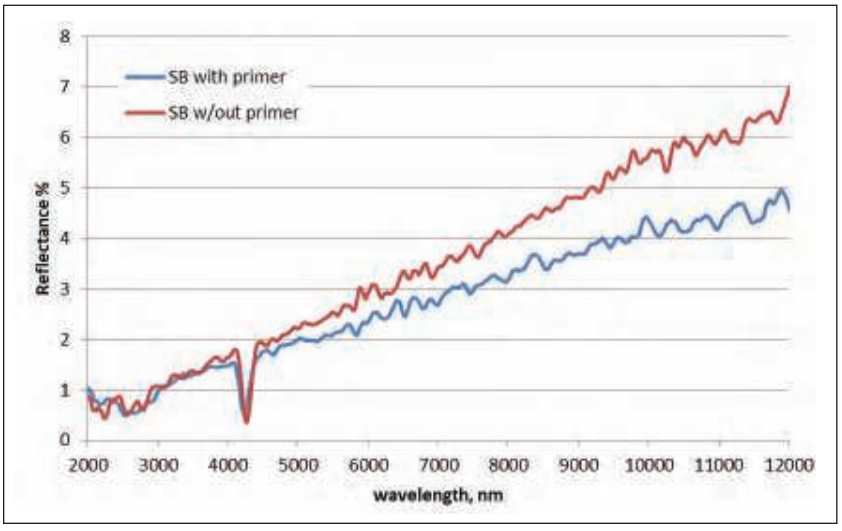

FIGURE 8—DRIFTS data for Singularity Black coatings on Al with and without primer.

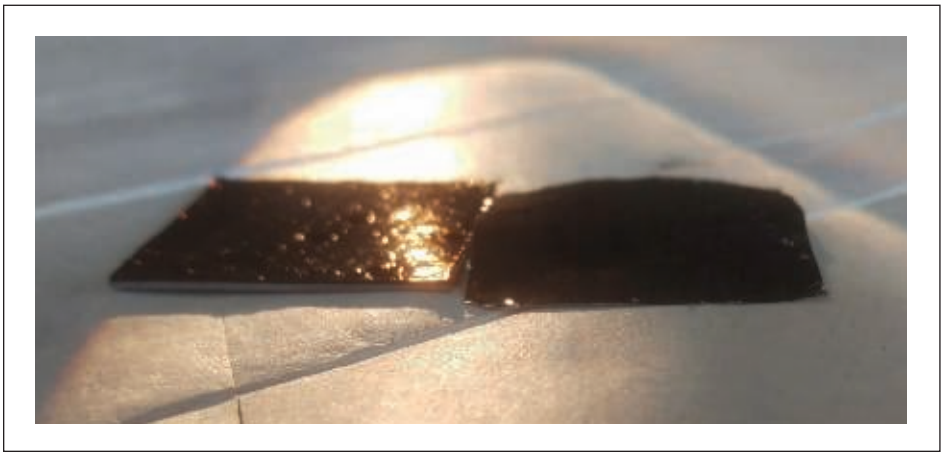

FIGURE 9—Glare at low angles of incidence can be seen in standard processed VANTA (L) but not with the sprayed coating (R), owing to its random structure.

μm. The data for CVD-grown VANTA arrays is presented in *Figure 7*, and the corresponding data for the Singularity coating is given in *Figure 8*.

The grazing-angle properties of these films is evident in the images given in *Figure 9*. A full bidirectional reflectance distribution function (BRDF) study of these coatings is underway.

RESULTS AND CONCLUSIONS

The THR of aligned arrays of CNTs can clearly be less than 1% in the visible, but it was troubling that VANTAs perform poorly at grazing angle.[4] The use of a nonaligned nanotube structure, such as the sprayed coating, was expected to improve grazing-angle performance without a significant increase in reflectivity. The sprayed coatings showed THR around 1% in the visible. To compare this to the theoretical value, we calculated the refractive index of the composite to be

$$n_{composite} = n_{air}Vf_{air} + n_{CNT}Vf_{CNT} \quad (6)$$

As a first assumption, the refractive index that was calculated for CNT at 45° was used as the value for that of

randomly aligned CNT. Using this assumption, coupled with the volume fraction (Vf) of CNT that was estimated by SEM (~0.2), an estimate for the refractive index of the entire composite ($n_{composite}$=1.2) was calculated. Returning to eq 1, the reflectance R of the interface between air and the composite can be calculated, and is 1.1%. This is in good agreement with the total reflectance data collected, ~1% at 550 nm. Thus, a 99% absorbing coating can be prepared using unaligned, porous CNT structures such as the sprayed coating developed in this work.

While not quantitative, the grazing-angle images show that the sprayed composite has hugely reduced glare compared to VANTA structures. Quantification of this effect using a variable angle setup in a UV-Vis-NIR spectrophotometer is planned as a next step in this investigation.

In conclusion, using the morphological and physical characteristics of CNTs, it was possible to create a black coating material with a more isotropic behavior, especially at grazing angles. This came at the loss of some performance, degrading the achieved THR by ~1% in the visible, and higher in the IR. The IR degradation may have been thickness-related (i.e., a thicker coating than that applied (~4 μm) would likely have performed better.

However, the creation of a paint-based alternative to VANTA coatings offers several key advantages. The thermal CVD process requires cleanroom catalyst deposition, typically via sputtering, and >700 °C temperatures for synthesis. These limit the materials and sizes of components that can be coated with this exceptional black. Materials like plastics and aluminum and other composites cannot host an aligned array. However, a sprayable version:

- can be applied to any substrate that can withstand 120 °C;
- is more amenable to large-area application; and
- does not require clean room catalyzation.

In conclusion, the Singularity coating, in addition to having good performance (~1% reflectance in the visible) and better low-angle performance, is easier to deposit on a larger number of substrates and is more readily scaled. Further optimization of this coating may lead to improvements in its performance. ❊

References

1. McCoy, D. E.; Feo, T.; Harvey, T. A., et al. Structural Absorption by Barbule Microstructures of Super Black Bird of Paradise Feathers. *Nat Commun*. 2018, *9*, 1. DOI:10.1038/s41467-017-02088-w
2. Kataura, H.; Kumazawa Y.; Maniwa, Y.; Umezu, I.; Suzuki, S.; Ohtsuka, Y.; Achiba, Y. Optical Properties of Single-Wall Carbon Nanotubes. *Synthetic Metals*. 1999, *103*, 2555-2558. DOI: 10.1016/S0379-6779(98)00278-1
3. Bao, H.; Ran X.; Fisher, T. Optical Properties of Vertical Arrays of Multiwalled Carbon Nanotubes from FTDT Simulations. *Optics Express*. 2010, *18*, 6, 6353.
4. Mizuno, K.; Ishii, J.; Kishida, H.; Hayamizu, Y.; Yasuda, S.; Futaba, D.; Yumura, M.; Hata, K. A Black Body Absorber from Vertically Aligned Single-Walled Carbon Nanotubes. *PNAS*. 2009, *106*, 15, 6044-6047.

D. CARNAHAN and **T. MORGAN**, NanoLab, Inc., 22 Bedford Street, Waltham, MA 02453; dcarnahan@nano-lab.com.